

for $\text{PdC}_{14}\text{H}_{13}\text{N}_2\text{ClSO}$ (**4c**): C, 42.12; H, 3.26; N, 7.02. Found: C, 41.90; H, 3.23; N, 6.83. Calcd for $\text{PdC}_{14}\text{H}_{13}\text{N}_2\text{ClSO}$ (**4d**, α and β isomers): C, 42.12; H, 3.26; N, 7.02. Found: C, 42.16; H, 3.22; N, 6.83.

Chloro(2-(methylsulfinyl)phenyl)-5-methyl-2-phenolato-O,N,S) palladium(II), α Isomer (5d α**).** An ethanolic solution (25 mL) of 2-(methylsulfinyl)-2'-hydroxy-5'-methylazobenzene (**6**) (100 mg, 0.36 mmol) was added to an ethanolic solution (25 mL) of Na_2PdCl_4 (150 mg, 0.50 mmol). When the mixture was stirred, the color of the solution gradually changed from yellow-brown to pink-violet. Stirring was continued for 8 h, and the solution was then evaporated in vacuo. The maroon powder was washed with water (3×5 mL) and then with 50% aqueous ethanol (3×5 mL). The dichloromethane extract (3×5 mL) of the solid was next subjected to chromatography on a silica gel column (45×1 cm) prepared in benzene. The light orange band of unreacted ligand was eluted first by using benzene as eluant. The required complex (**5d α**) was then eluted as a pink-violet band by an acetonitrile-benzene (1:9) mixture. Evaporation of the eluant left a solid residue, which was recrystallized from a dichloromethane-methanol mixture (3:1; 15 mL), affording dark violet crystals in 90% yield. Anal. Calcd for $\text{PdC}_{14}\text{H}_{13}\text{N}_2\text{SO}_2\text{Cl}$ (**5d α**): C, 40.50; H, 3.13; N, 6.75. Found: C, 40.45; H, 3.10; N, 6.70.

Oxidation of **4a to **5a** by mCPBA.** To a chloroform solution (30 mL) of **4a** (100 mg, 0.27 mmol) was added dropwise with magnetic stirring a solution of mCPBA (90 mg, 0.39 mmol) in the same solvent (20 mL). The reaction mixture was stirred for 4 h. The color of the solution was changed from brown-red to pink-violet. After the completion of the reaction, the solvent was evaporated to dryness in vacuo. The residue was thoroughly washed with 50% aqueous ethanol (5×3 mL) and then with diethyl ether (3×3 mL) to remove any unreacted mCPBA and its reduced product mCBA. The dichloromethane solution (10 mL) of the residue was then chromatographed over a silica gel column (45×1 cm) made in benzene. The pink-violet band of **5a** was eluted by an acetonitrile-benzene (1:9) mixture. Evaporation of this solution in vacuo gave the dark violet solid compound in 85% yield. Anal. Calcd for $\text{PdC}_{13}\text{H}_{11}\text{N}_2\text{SO}_2\text{Cl}$ (**5a**): C, 38.92; H, 2.74; N, 6.99. Found: C, 38.98; H, 2.71; N, 6.90.

The oxidations of **4b** to **5b**, **4c** to **5c** and **4d** to **5d α** were carried out similarly. Yields were respectively 84%, 80%, and 50%. In the case of **4d**, which consists of α and β isomers the oxidation product was also found to consist of a mixture. The oxidized solution (after removing mCPBA and mCBA) when subjected to column chromatography first afforded the pink-violet band of **5d α** . The second pink-violet band followed, but it furnished only a gummy mass that could not be purified. Anal. Calcd for $\text{PdC}_{15}\text{H}_{13}\text{N}_2\text{SO}_2\text{Cl}$ (**5d**): C, 47.81; H, 3.15; N, 5.87. Found: C, 48.01; H, 3.18; N, 5.90. Calcd for $\text{PdC}_{14}\text{H}_{13}\text{N}_2\text{SO}_2\text{Cl}$ (**5c**):

C, 40.50; H, 3.13; N, 6.75. Found: C, 40.46; H, 3.11; N, 6.70. Calcd for $\text{PdC}_{14}\text{H}_{13}\text{N}_2\text{SO}_2\text{Cl}$ (**5d α**): C, 40.50; H, 3.13; N, 6.75. Found: C, 40.40; H, 3.10; N, 6.70.

Demetalation of **5d α to **6**.** To an acetonitrile solution (20 mL) of **5d α** (60 mg, 0.14 mmol) was added dropwise with magnetic stirring a solution of 99% hydrazine hydrate (75 mg) in the same solvent (2 mL). The reaction mixture was stirred for 0.5 h. The color of the solution changed from pink-violet to orange-yellow, and metallic palladium precipitated. The solution was filtered, and the filtrate was evaporated in vacuo. The gummy residue was dissolved in dichloromethane (5 mL) and subjected to chromatography on a silica gel column (40×1 cm) prepared in petroleum ether. An orange-yellow band was eluted with benzene. The eluant on evaporation in vacuo gave **6** in pure form (mp 132 °C) in 89% yield. Anal. Calcd for $\text{C}_{14}\text{H}_{14}\text{N}_2\text{SO}_2$: C, 61.31; H, 5.11; N, 10.22. Found: C, 61.25; H, 5.05; N, 10.18. The compound so obtained was identical in all respects with the compound synthesized by hydrogen peroxide oxidation of the corresponding thioether (vide supra).

Kinetic Measurements. Thermostated solutions of reactants were mixed, diluted to required volumes, and transferred to an absorption cell of 1 cm path length. Increase in absorption of the reactants at 540 nm was digitally recorded as a function of time. A_α was measured when intensity changes leveled off. In all experiments the concentration of mCPBA was kept high so as to maintain pseudo-first-order conditions. Values of pseudo-first-order rate constants (k_{obsd}) were obtained from the slopes of the plots of $-\ln(A_\alpha - A_\infty)$ vs t lines. Values of second-order rate constants, k , were obtained from the slopes of the plots of k_{obsd} vs [mCPBA]. Activation parameters were obtained from the Eyring equation. Values of k_{obsd} , k , H^\ddagger , and S^\ddagger and their deviations were calculated by using the usual least-squares methods.²⁹ A minimum of 30 A_t - t data points were used in each calculation.

Acknowledgment is made for financial support received from the Council of Scientific and Industrial Research and Department of Science and Technology, New Delhi, India.

Registry No. **3a**, 112945-72-9; **3b**, 112945-73-0; **3c**, 112945-74-1; **3d**, 112945-75-2; **4a**, 112968-76-0; **4b**, 112968-77-1; **4c**, 112968-78-2; **4d α** , 112968-79-3; **4d β** , 112968-80-6; **5a**, 112968-81-7; **5b**, 112968-82-8; **5c**, 112968-83-9; **5d α** , 112945-77-4; **6**, 112945-76-3; Na_2PdCl_4 , 13820-53-6; 2-(methylthio)azobenzene, 101418-85-3; 2-(benzylthio)azobenzene, 101418-87-5; 2-(methylthio)-4'-methylazobenzene, 101418-86-4; 2-(methylthio)-5'-methylazobenzene, 102073-18-7; 2-(methylthio)-2'-hydroxy-5'-methylazobenzene, 85261-27-4.

(29) Youden, W. J. *Anal. Chem.* **1947**, *19*, 946-950.

Contribution from the Laboratorium für Anorganische Chemie, ETH-Zentrum, CH-8092 Zürich, Switzerland, and Istituto di Chimica Farmaceutica, Università di Milano, Viale Abruzzi, 42, I-20131 Milano, Italy

Platinum(II) Phosphine Complexes Containing 1,3,5-Triazine and Related Ligands

Werner Kaufmann,^{1a} Luigi M. Venanzi,^{*1a} and Alberto Albinati^{1b}

Received September 15, 1987

Solution studies of the complexes $[\text{PtCl}_2(\text{PET}_3)]_n$ -1,3,5-triazine ($n = 1-3$), $[\text{PtCl}_2(\text{PR}_3)]_n$ -pyrimidine ($\text{R} = \text{Et}, n\text{-Bu}; n = 1, 2$), and *trans*- $\text{PtCl}_2\text{L}(\text{PR}_3)$ ($\text{L} = \text{pyridine}, 4\text{-chloropyridine}; \text{R} = \text{Et}, n\text{-Bu}$) are reported. It is shown that (a) coordination of the " $\text{PtCl}_2(\text{PR}_3)$ " fragment does not greatly weaken the donor capacity of the still-uncoordinated nitrogen atom of the heterocycle and (b) these complexes are dynamic in solution and the degree of lability increases in the order pyridine < pyrimidine < 1,3,5-triazine. The X-ray crystal structure of $[\text{PtCl}_2(\text{PET}_3)]_3$ -1,3,5-triazine was determined. The crystals are triclinic and belong to the space group $P\bar{1}$ with unit cell dimensions $a = 13.020$ (3) Å, $b = 13.098$ (2) Å, $c = 13.251$ (2) Å, $\alpha = 62.75$ (1)°, $\beta = 65.95$ (2)°, $\gamma = 75.49$ (2)°, $V = 1828.8$ (1) Å³, and $Z = 2$. The structure was refined to $R = 0.036$. Each platinum atom shows normal square-planar geometry with bonding parameters that are typical for compounds of the type *trans*- $\text{PtCl}_2(\text{N-ligand})(\text{PR}_3)$. There does not appear to be any significant change in the triazine structural parameters upon coordination.

Introduction

The coordination chemistry of 1,3,5-triazine (tri) has been investigated very little. The first reported complex appears to be $[\text{Ru}(\text{NH}_3)_5(\text{tri})](\text{ClO}_4)_2$, described in 1968 by Ford et al.² In

a later publication, Allenstein et al.³ reported some "addition products" of the composition $(\text{SbCl}_5)_2(\text{tri})$, $\{\text{TiCl}_4(\text{tri})\}_x$, $\text{SbCl}_5(\text{tri})$, $\text{TiCl}_4(\text{tri})_2$, $\text{AlCl}_3(\text{tri})$, $\text{AlCl}_3(\text{tri})_2$, and $\text{SnCl}_4(\text{tri})_2$. The first two complexes seem to be the only compounds described so far in which tri coordinates to more than one metal center. All subsequent

(1) (a) ETH-Zentrum. (b) Università di Milano.

(2) Ford, P.; Rudd, D. P.; Gaunder, R.; Taube, H. J. *Am. Chem. Soc.* **1968**, *90*, 1187.

(3) Allenstein, E.; Beyl, V.; Löhmar, K. Z. *Anorg. Allg. Chem.* **1971**, *381*, 40.

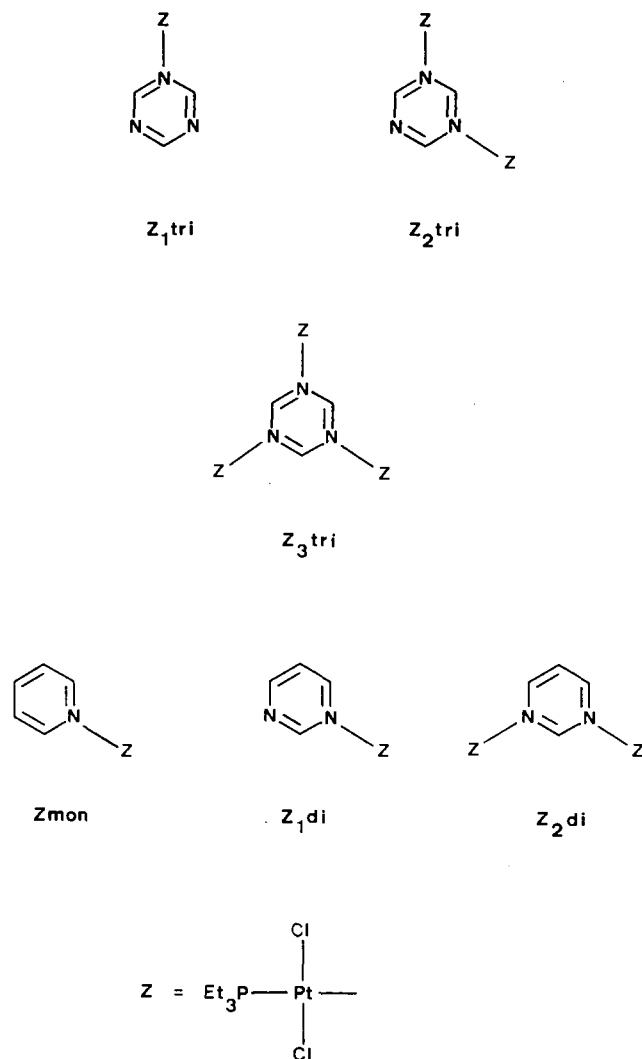
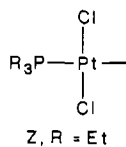


Figure 1. Azine complexes with the notations shown in the text.

publications⁴⁻¹¹ deal with tri as a monocoordinating ligand.

During our studies of discrete polynuclear complexes, we began an investigation of the coordination chemistry of tri because of the presence of three potential nonchelating donor atoms in this molecule. It was also expected that this study would provide information about electronic changes occurring within the heterocyclic ring upon successive coordination of metal centers.

In order to gain some basic information, particularly about the latter problem, a simple metal fragment was chosen, namely

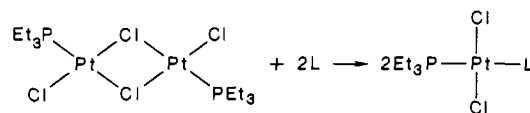


as the ³¹P and ¹⁹⁵Pt NMR data of the resulting tri complexes would allow their easy structural characterization in solution.

Results and Discussion

Preliminary investigations indicated that different species were simultaneously present in solution and that dynamic processes were occurring on the NMR time scale. Thus the coordination behavior of triazine was first studied in solution.

The complexes observed are shown in Figure 1. They are all of the type *trans*-PtCl₂L(PEt₃) (Z_nL (n = 1-3); L = nitrogen donor) and are conveniently prepared, as are other compounds of the same type, by the bridge-splitting reaction¹²



(Z₂ + 2L → 2ZL), which gives exclusively products of *trans* configuration because of the moderately high *trans* effect of the tertiary phosphine and the low *trans* effect of the nitrogen ligand.¹³⁻¹⁶

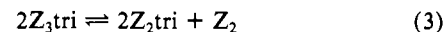
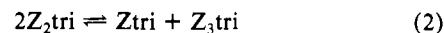
Equilibria in Solution. Solutions of the complexes Ztri, Z₂tri, and Z₃tri were prepared by adding the appropriate stoichiometric amount of tri to CDCl₃ or CD₂Cl₂ solutions of Pt₂Cl₄(PEt₃)₂ (Z₂). The species present were characterized through their ¹H and ³¹P NMR spectra. These will be discussed in detail later. Routine monitoring of the reactions was done by following changes in the ³¹P NMR spectra on addition of the nitrogen base to the binuclear platinum complex.

Solutions of complexes containing either 1,3-diazine (pyrimidine, di), Zdi and Z₂di, or pyridine (mon), Zmon, were similarly prepared.

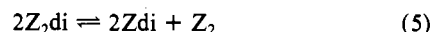
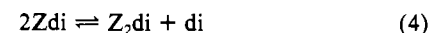
When 1,3,5-triazine (tri) was used as a ligand, the species shown in Scheme Ia were observed. The equilibria between them are conveniently expressed by eq 1-3. Although numerous other equilibria can be envisaged, those given there are sufficient for an unambiguous definition of the system in question.

Scheme I

(a) solution equilibria for platinum-triazine complexes



(b) solution equilibria for platinum-pyrimidine complexes



At room temperature it was found that (a) in solutions containing Z:triazine ratios of 1:1 equilibrium 1 was established with nearly complete formation of Ztri, (b) in solutions containing Z:triazine ratios of 2:1 equilibrium 2 was established with almost complete formation of Z₂tri, and (c) in solutions containing Z:triazine ratios of 3:1 equilibrium 3 was established, almost equal amounts of Z₃tri and Z₂tri being present in solution (see Figure 2a).

It was also found that while equilibria 1 and 2 are only slightly shifted toward the left upon cooling to -60 °C, equilibrium 3 is shifted almost completely to the left upon cooling of the solution to this temperature (see Figure 2b).

These observations are conveniently discussed in terms of the successive formation constants given in Scheme Ia. Observations a and b, coupled with the near temperature independence of the equilibria, indicate that coordination of the first platinum atom to triazine does not cause major changes in the donor capacity of the other potential nitrogen donors. It should be noted that equilibrium 3 in Scheme Ia and equilibrium 8 in Scheme IIa

- (4) Wöhrle, D. *Makromol. Chem.* **1974**, *175*, 1751.
- (5) Johnston, R. D.; Vagg, R. S.; Watton, E. C. *Inorg. Chim. Acta* **1977**, *22*, L37.
- (6) Johnston, R. D.; Vagg, R. S.; Watton, E. C. *Inorg. Chim. Acta* **1978**, *26*, 103.
- (7) Haas, O.; von Zelewsky, A. *J. Chem. Res., Synop.* **1980**, 77.
- (8) Haas, O.; von Zelewsky, A. *J. Chem. Res., Synop.* **1980**, 78.
- (9) Brodersen, K.; Hoffman, J.; Erdmann, R. *Z. Anorg. Allg. Chem.* **1981**, *482*, 217.
- (10) Walker, F. A.; Reis, D.; Balke, V. L. *J. Am. Chem. Soc.* **1984**, *106*, 6888.
- (11) Boyer, A.; Fazakerley, G. V. *J. Inorg. Nucl. Chem.* **1981**, *43*(8), 1955.

- (12) Chatt, J.; Venanzi, L. M. *J. Chem. Soc.* **1955**, 3858.
- (13) Chatt, J.; Duncanson, L. A.; Venanzi, L. M. *J. Chem. Soc.* **1955**, 4456.
- (14) Langford, C. H.; Gray, H. B. *Ligand Substitution Processes*; W. A. Benjamin: New York, 1965.
- (15) Basolo, F.; Pearson, R. G. *Mechanism of Inorganic Reactions*; Wiley: New York, 1967.
- (16) Burdett, J. K. *Inorg. Chem.* **1977**, *16*, 3013.

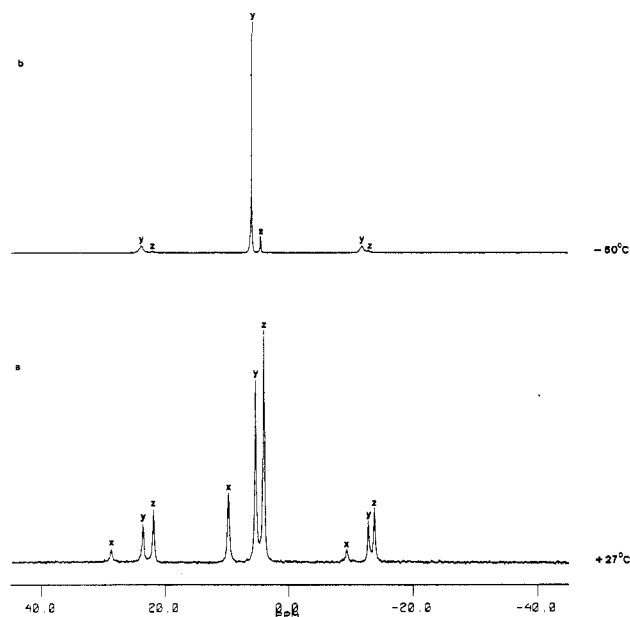
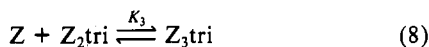
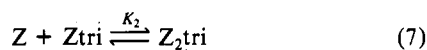
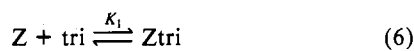


Figure 2. 101.3-MHz $^{31}\text{P}\{^1\text{H}\}$ NMR spectra of CD_2Cl_2 solutions obtained from $\text{Pt}_2\text{Cl}_4(\text{PEt}_3)_2$ and triazine in the ratio 3:2: (a) 27 °C; (b) -60 °C. The resonances denoted by x are due to $\text{Pt}_2\text{Cl}_4(\text{PEt}_3)_2$, those denoted by y are due to Z_3tri , and those denoted by z are due to Z_2tri .

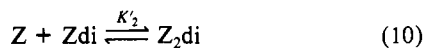
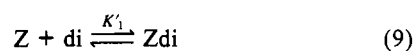
represent the same reaction. Equilibrium 3, unlike those represented by eq 1 and 2, involves different numbers of particles of reactants and products, two and three, respectively, and thus, equilibrium 3 is expected to be strongly temperature-dependent because of the contribution of the $T\Delta S$ term to the value of ΔG . However, the fact that at low temperatures the formation of Z_3tri is almost complete even when the Z:triazine ratio is 3:1 indicates that although two platinum atoms are already bonded to triazine the donor capacity of its remaining free nitrogen atom is not weakened to the extent of preventing its coordination.

Scheme II

(a) successive formation equilibria for platinum-triazine complexes



(b) successive formation equilibria for platinum-pyrimidine complexes

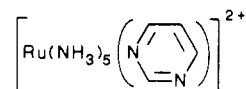


A similar type of behavior has also been observed for pyrimidine (di), which forms the complexes Zdi and Z_2di . In this case as well, the following observations were made. (a) When the Z:pyrimidine ratio was 1:1, equilibrium 4 was established with nearly complete formation of Zdi. (b) When the Z:pyrimidine ratio was 2:1, only Z_2di could be detected; i.e., equilibrium 5 is shifted completely to the left. Furthermore, the product distribution is practically temperature-independent.

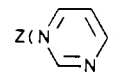
The above data can be interpreted analogously to those for the triazine complexes, i.e., in terms of Scheme IIb. It is, however, surprising that no Zdi is detectable in solutions having a 2:1 Z:di ratio, as one might have expected the occurrence of disproportionation reaction 5, which corresponds to reaction 3 in the triazine system.

The observation that coordination of one transition-metal fragment to a diazine does not drastically change the basicity of

the second nitrogen atom is not without precedent. Thus, it has been reported² that the $\text{p}K_a$ value of the pyrimidine complex

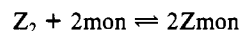


is ca. 0 while the $\text{p}K_{a1}$ value for the protonation of the free base is 1.3.¹⁷ This decrease in basicity has been attributed to electrostatic effects.² As our platinum Lewis acid Z is uncharged, one might expect the $\text{p}K_a$ of



to be comparable with that of the free base. Thus, it is not surprising that the formation of Z_2di is quantitative and that Z_3tri is easily and, at least at low temperatures, quantitatively formed. (A direct measurement of the $\text{p}K$ values of free and coordinated 1,3,5-triazine is not possible as it decomposes in acidic solution.)

The binuclear complexes $\text{Pt}_2\text{Cl}_4(\text{PR}_3)_2$ (Z_2) react quantitatively also with monodentate heterocyclic amines (L), giving *trans*- $\text{PtCl}_2(\text{L})(\text{PR}_3)$ (ZL).¹² Thus, *trans*- $\text{PtCl}_2(\text{mon})(\text{PEt}_3)$ was obtained as described previously.¹⁸ The ^1H and ^{31}P NMR spectra of solutions of this complex do not show the presence of either the binuclear complex Z_2 or the pyridine, "mon". Thus the equilibrium



is completely shifted to the right. As will be shown later, however, this system is dynamic in solution.

Dynamic Behavior. The ^1H and ^{31}P NMR spectra of all the complexes indicate that dynamic processes occur in solution. An example, typical for the behavior of the tri complexes, is that shown in Figure 3, where the dominant species present is Z_3tri . As can be seen there, at room temperature the signals due to the aromatic protons are very broad but sharpen below -20 °C. Examination of the temperature dependence of the ^1H NMR spectra of Ztri , Z_2tri , and Z_3tri shows that the activation energies for the dynamic behavior of these species are comparable as shown by the temperature at which sharp spectral lines first appear, e.g., -20 to -40 °C for Z_2tri (see Figure 3). Sharp resonances first appear in the same temperature range also in Ztri and Z_3tri . The ^{31}P 2-D exchange spectrum of a solution containing Z_3tri in equilibrium with Z_2tri and Z_2 (eq 3) at 27 °C clearly shows cross peaks indicating exchange between all the species present in solution (see Figure 4). This provides additional evidence in support of a slow process that exchanges the ^{31}P environments in Z_3tri , Z_2tri , and Z_2 . Further evidence of dynamic behavior is provided by the following.

(a) The ^{13}C NMR spectrum of the aromatic region of Z_3tri , at room temperature, shows only one signal that is broader than the signals due to the phosphine carbon atoms.

(b) The room-temperature ^1H NMR spectrum in the aromatic region of Z_2tri shows two very broad signals at 9.89 and 10.33 ppm, which have been assigned to H^b and H^a , respectively (see Figure 3). (Proton-proton magnetization-transfer experiments confirmed the above assignments and showed that the two sites were exchanging.)

The pyrimidine complexes Zdi and Z_2di are also dynamic in solution. However, their ^1H NMR spectra indicate that the activation energy for this exchange is somewhat higher than in the case of the triazine complexes. As can be seen in Figure 5, sharp spectra are already obtained at 0 °C. The complexes Zdi and Z_2di appear to exchange at comparable rates, as in both cases sharp lines are first observable in the same temperature range.

The occurrence of exchange processes can be easily studied even when only one species can be detected in solution. Thus, when $\text{Pt}_2\text{Cl}_4(\text{PEt}_3)_2$ and di are present in a 1:1 ratio, the ^{31}P NMR

(17) Albert, A.; Goldacre, R.; Philips, J. *J. Chem. Soc.* **1948**, 2240.

(18) Hitchcock, P. B.; Jacobson, B.; Pidcock, A. *J. Chem. Soc., Dalton Trans.* **1977**, 2038.

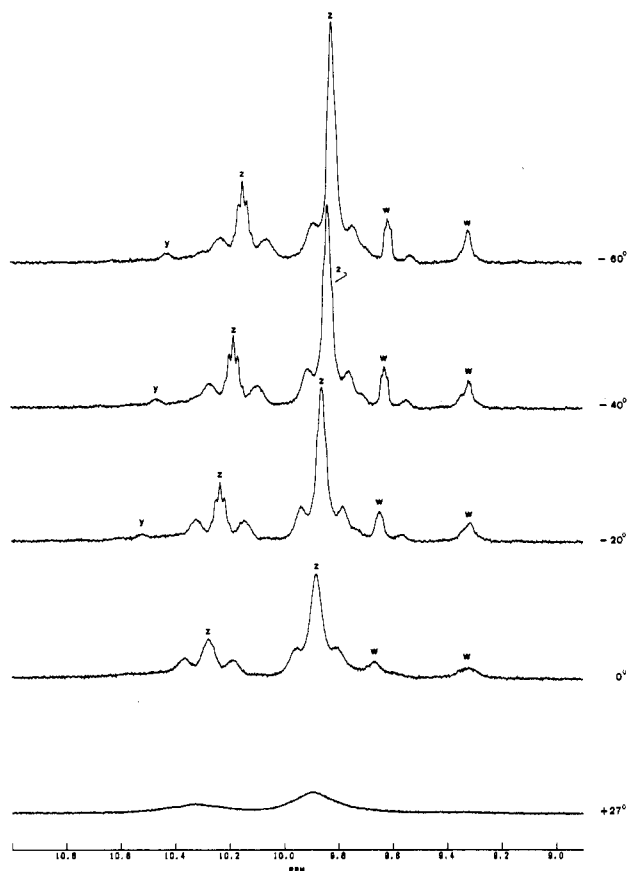


Figure 3. Temperature dependence of the 90-MHz ^1H NMR spectrum of the aromatic protons of a CD_2Cl_2 solution obtained from $\text{Pt}_2\text{Cl}_4(\text{PEt}_3)_2$ and triazine in the ratio 1:1. The resonances denoted by y are due to Z_3tri , those denoted by w are due to Ztri , and those denoted by z are due to Z_2tri .

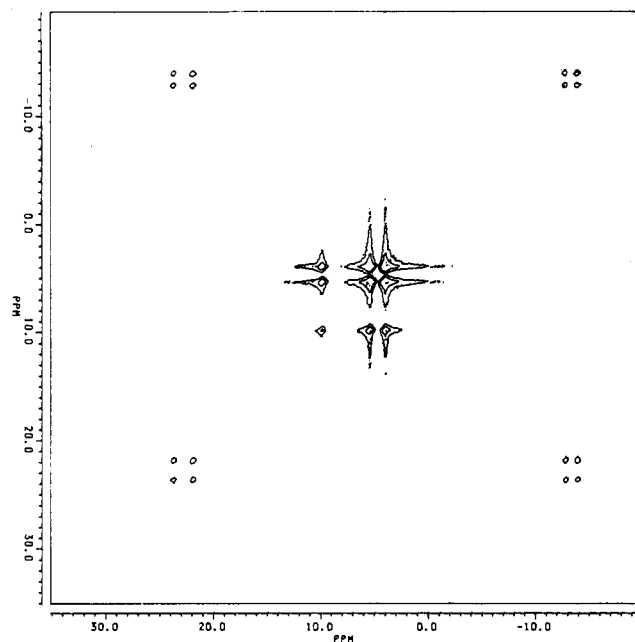


Figure 4. ^{31}P 2-D exchange spectrum of a solution of crystalline Z_3tri .

spectrum shows only the presence of Z_2di in this solution. However, addition of 1 equiv of $\text{Pt}_2\text{Cl}_4(\text{P-}n\text{-Bu}_3)_2$ to 1 equiv of Z_2di to this solution leads to the rapid formation of a mixture containing statistical amounts of $\text{Pt}_2\text{Cl}_4(\text{P-}n\text{-Bu}_3)_2$, $\text{Pt}_2\text{Cl}_4(\text{PEt}_3)_2$, $\text{Pt}_2\text{Cl}_4(\text{PEt}_3)(\text{P-}n\text{-Bu}_3)$, $(\text{PEt}_3)\text{Cl}_2\text{Pt}(\mu\text{-di})\text{PtCl}_2(\text{PEt}_3)$, $(\text{PEt}_3)\text{Cl}_2\text{Pt}(\mu\text{-di})\text{PtCl}_2(\text{P-}n\text{-Bu}_3)$, and $(\text{P-}n\text{-Bu}_3)\text{Cl}_2\text{Pt}(\mu\text{-di})\text{PtCl}_2(\text{P-}n\text{-Bu}_3)$. It should be pointed out here, however, that the binuclear species $\text{Pt}_2\text{Cl}_4(\text{PR}_3)_2$ also undergo easy exchange as shown by

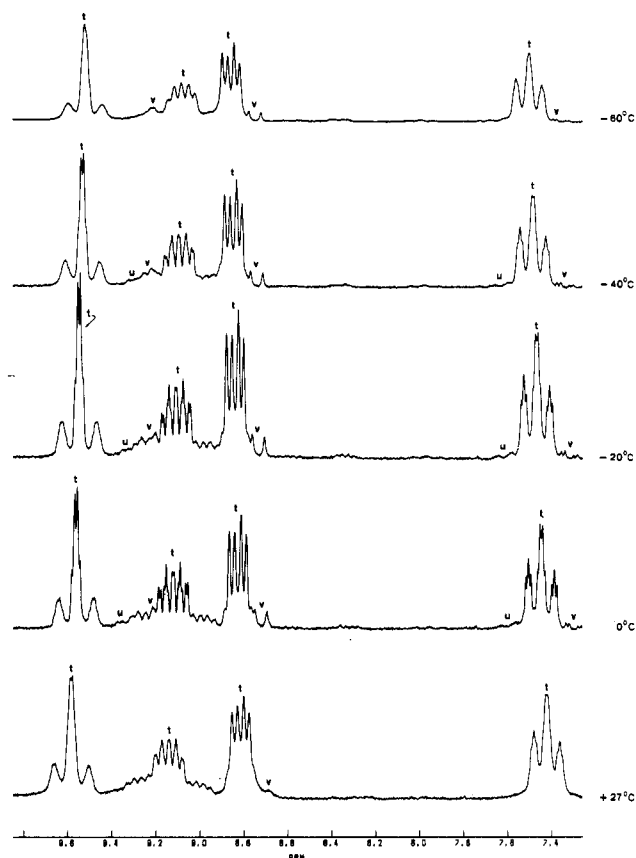


Figure 5. Temperature dependence of the 90-MHz ^1H NMR spectrum of the aromatic protons of a solution obtained by dissolving $\text{Pt}_2\text{Cl}_4(\text{PEt}_3)_2$ and pyrimidine (di) in the ratio 2:1 in CD_2Cl_2 . The resonances denoted by t are due to Zdi , those denoted by u are due to Z_2di , and those denoted by v are due to free di.

mixing equimolar amounts of $\text{Pt}_2\text{Cl}_4(\text{PEt}_3)_2$ and $\text{Pt}_2\text{Cl}_4(\text{P-}n\text{-Bu}_3)_2$, which gives a mixture containing the starting material as well as $\text{Pt}_2\text{Cl}_4(\text{PEt}_3)(\text{P-}n\text{-Bu}_3)$ in statistical amounts. Disproportionation reactions of this type have been reported¹⁹ for mixtures of $\text{Pt}_2\text{Cl}_4(\text{P-}n\text{-Bu}_3)_2$ and $\text{Pd}_2\text{Cl}_4(\text{P-}n\text{-Bu}_3)_2$.

Experiments of the type described above show that even complexes such as *trans*- $\text{PtCl}_2(\text{mon})(\text{PR}_3)$ are dynamic in solution. Thus, addition of a solution of $\text{Pt}_2\text{Cl}_4(\text{P-}n\text{-Bu}_3)_2$ to a solution of *trans*- $\text{PtCl}_2(\text{mon})(\text{PEt}_3)$ produced a mixture containing the three bridged complexes mentioned above, the original pyridine complex, and *trans*- $\text{PtCl}_2(\text{mon})(\text{P-}n\text{-Bu}_3)$ in statistical amounts. It should be noted, however, that the proton spectra of the pure pyridine complexes are quite sharp at room temperature and thus these species are less dynamic than the corresponding complexes of pyrimidine (di) and 1,3,5-triazine (tri).

From a mechanistic standpoint, reactions 1, 2, and 4 are best formulated as being of $\text{S}_{\text{N}}2$ type, as is generally the case for nucleophilic substitutions at platinum(II) square-planar complexes.¹⁴⁻¹⁶ This is because the species concerned, Ztri , Z_2tri , and Zdi , all contain uncoordinated nitrogen atoms that can act as "external nucleophiles". A possible mechanistic pathway for the exchange shown in equilibrium 1 is shown in Figure 6. Reaction 2 could be described by a pathway analogous to that shown in Figure 6 substituting Ztri by Z_2tri , Z_3tri by Z_3tri , and tri by Ztri . A similar description could apply to reaction 4. As implied there, the sequence of reactions A-D in Figure 6 is formally equivalent to the donor "self-exchange" reaction within Z_2tri shown in Figure 7. The occurrence of such "donor exchange" processes is supported by the observations made earlier under (a) and (b).

Magnetization-transfer experiments of the type described for Z_2tri were carried out on Ztri and Zdi , showing that also in these

(19) Kiffen, A. A.; Masters, C.; Visser, J. P. J. *Chem. Soc., Dalton Trans.* **1975**, 1311.

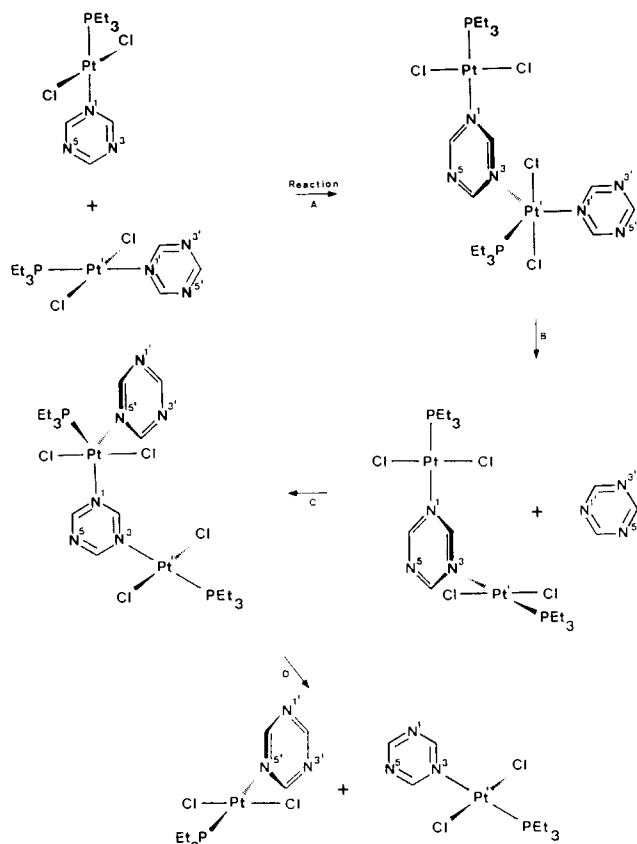


Figure 6. Possible mechanistic pathway for the donor-site exchange in Ztri.

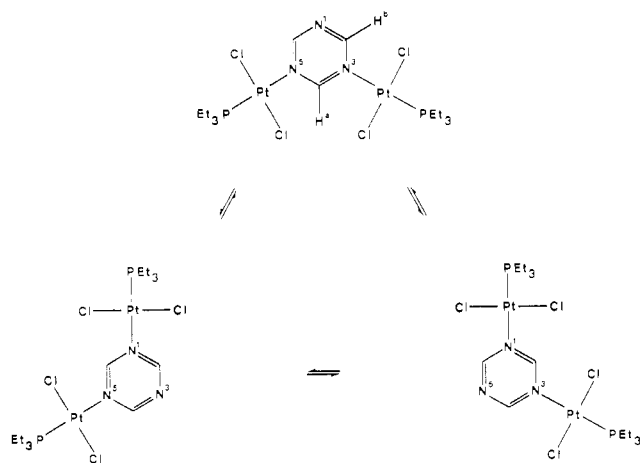
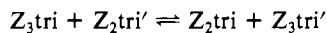


Figure 7. The formal donor-site exchange in Z₂tri.

cases "donor exchange" processes are taking place.

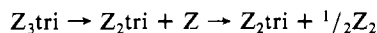
An interpretation of the dynamic behavior shown by solutions obtained by dissolving crystalline Z₃tri is more difficult. As mentioned earlier, the species shown in equilibrium 3 of Scheme 1a, i.e., Z₂, Z₂tri, and Z₃tri, are present in solution.

The reaction



can be easily envisaged as occurring by a pathway which is analogous to that described for Ztri in Figure 6.

The problem arises with the unambiguous interpretation of the initial step, which, starting from Z₃tri, leads to the formation of Z₂ and Z₂tri. A simple pathway could be envisaged by postulating a dissociative mechanism of the type



As dissociative mechanisms in square-planar platinum(II) com-

Table I. Comparison between the Solid-State and Solution ³¹P NMR Data^a of Z₂tri and Z₃tri

complex	solid state		soln ^b	
	δ	¹ J(Pt,P)	δ	¹ J(Pt,P)
Z ₂	14.5	3708	10.33	3843
Z ₂ tri	4.5	3556	4.48	3621
Z ₃ tri	8.2	3601	5.85	3694
	6.0	3638		
	3.0	3650		

^a¹J(Pt,P) values are in Hz. ^bMeasurements were made at room temperature.

plexes are still somewhat controversial, another possibility is provided by an S_N2-type reaction involving either the solvent (S, in this case CH₂Cl₂ or CHCl₃) or impurities in the solvent such as residual water:



One can also conceive an intramolecular pathway that leads directly to the formation of Pt₂Cl₄(PEt₃)₂ with concomitant formation of Ztri, which then reacts further with Z₃tri to give Z₂tri. This process is schematically shown in Figure 8a. However, the X-ray data on Z₃tri indicate that the distortions required to achieve a transition state of this type would be too large to be compatible with the observed low activation energy for this reaction. Thus, the structural parameters obtained for Z₃tri give a value of ca. 5.5 Å for the shortest possible approach between, e.g., Pt(1) and Cl(3). This is based on the assumption that there is free rotation about the Pt(2)-N(2) bond (see Figure 10) but no distortion of bond angles.

Yet another pathway is shown in Figure 8b. This is of the associative type, and the only major restriction is caused by the steric bulk of the two interacting units. Support for this hypothesis is provided by the reaction of *trans*-PtCl₂(mon)(P-*n*-Bu₃) with *trans*-PtCl₂(4-Cl-mon)(PEt₃), which gives a mixture of the starting materials as well as *trans*-PtCl₂(mon)(PEt₃) and *trans*-PtCl₂(4-Cl-mon)(L) (L = P-*n*-Bu₃ and PMePh₂) on standing for 2 h in solution at room temperature.

Finally we propose that also reaction 5 can be explained as done for reaction 3.

Isolated Complexes. As can be expected from the dynamic behavior described above, the isolation of the complexes described in the earlier sections poses problems. Attempts to obtain solid samples were made only for complexes containing PEt₃.

The isolation of Z₃tri posed no problems, as it is the least soluble component of the mixture.

Only oily residues could be obtained, by solvent evaporation under high vacuum, from solutions containing predominantly Ztri. These oils, when dissolved in solvents such as CDCl₃, gave again the original product mixture. Slow evaporation of such solutions, or of solvent mixtures, gave Z₃tri as the only solid. Solids of composition Z₂tri could be obtained only by rapid high-vacuum evaporation of the solvent from solutions containing predominantly this species. As, however, these solids could contain an equimolecular mixture of Ztri and Z₃tri, the solid-state ³¹P NMR spectra of Z₃tri and "Z₂tri" were recorded.

The solid-state ³¹P NMR spectrum of Z₃tri shows three main resonances accompanied by their respective ¹⁹⁵Pt satellites (see Table I and Figure 9). This splitting is likely to be due to the presence of three magnetically inequivalent phosphorus atoms in solid Z₃tri: Its X-ray crystal structure (see later) shows that the angles between the Z fragments and the tri plane are all different.

The ³¹P NMR spectrum of Z₂tri shows only one resonance flanked by its ¹⁹⁵Pt satellites (see Table I and Figure 9). As can be seen there, its NMR parameters differ from those of Z₃tri.

For the pyrimidine complexes, while Z₂di posed no isolation problems, the preparation of solid samples of Zdi failed as evaporation of solutions containing predominantly Zdi led to the rapid formation of Z₂di, presumably because of the high volatility of pyrimidine. Attempts to produce solids by precipitation also failed.

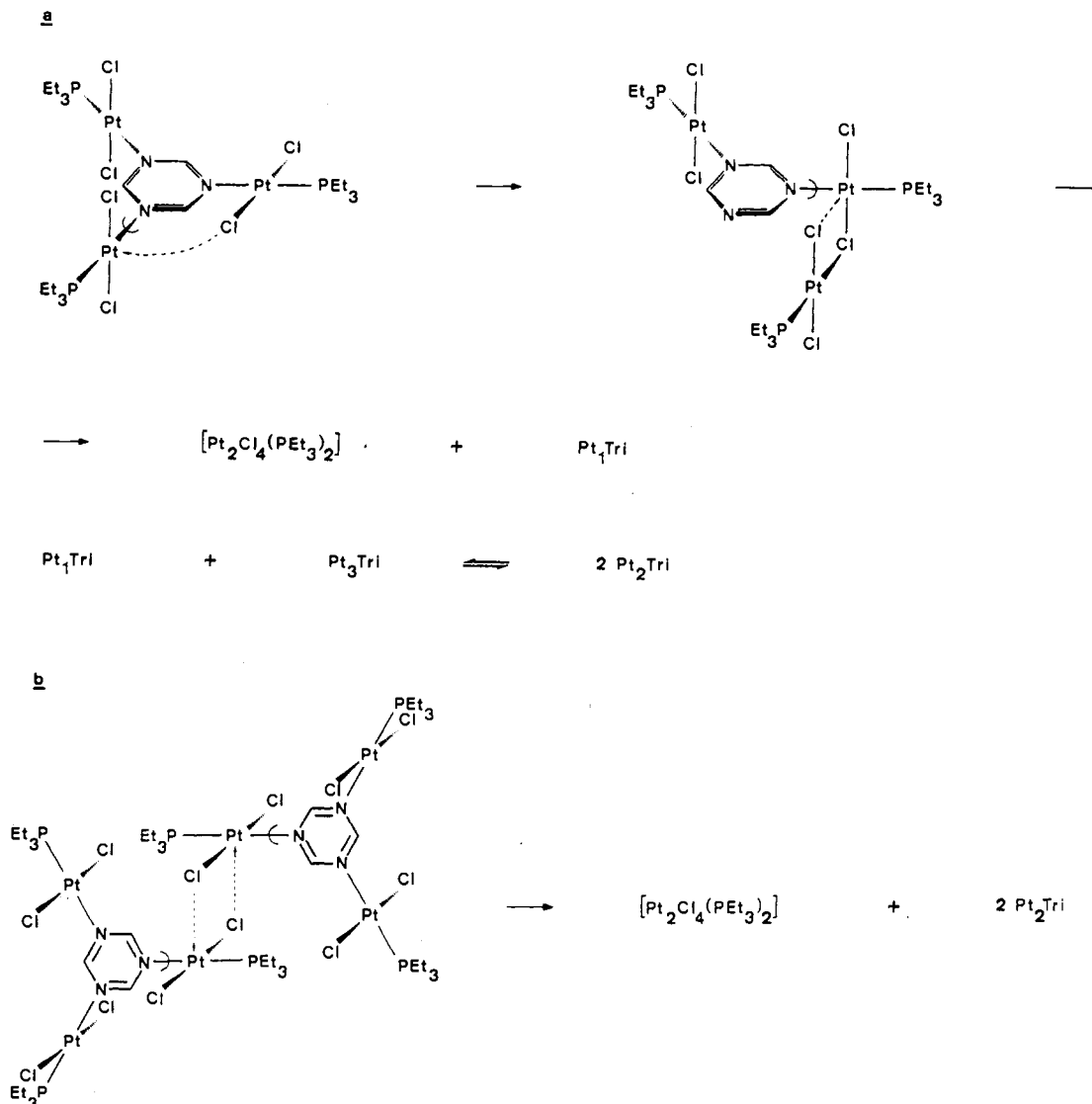


Figure 8. Some possible associative mechanistic pathways for the dynamic ligand-exchange processes observed in $Z_3\text{tri}$.

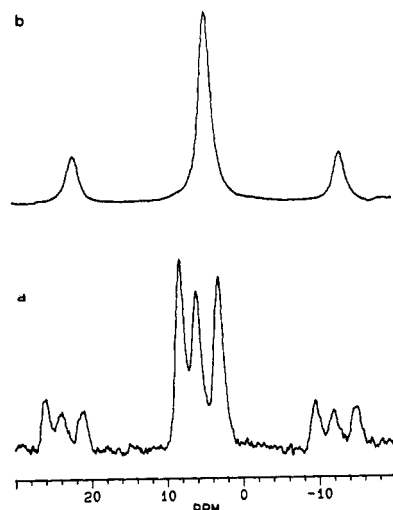


Figure 9. Solid-state ^{31}P MAS NMR spectra of $Z_3\text{tri}$ (a) and $Z_2\text{tri}$ (b).

^{31}P and ^{195}Pt NMR Spectra. The relevant data for the complexes $Z_n\text{L}$ ($Z = \text{PtCl}_2(\text{PEt}_3)$; $n = 1-3$; $L = \text{mon, di, and tri}$) are listed in Table II. The splitting of the binuclear platinum complex by a nitrogen heterocycle produces the expected²⁰ large upfield

Table II. ^{31}P and ^{195}Pt NMR Data^a for the Complexes $Z_n\text{L}$ ($Z = \text{PtCl}_2(\text{PEt}_3)$; $L = \text{mon, di, tri}$)

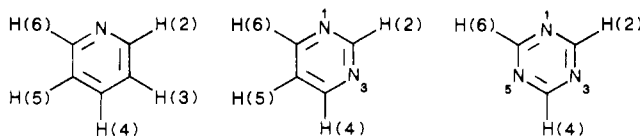
complex	$\delta(^{31}\text{P})^b$	$\delta(^{195}\text{Pt})^c$	$^1J(\text{Pt,P})$
Z_2	10.33	-3424	3843
Z_{mon}	-0.29	-3571	3350
Z_{di}	1.41	-3610	3443
$Z_2\text{di}$	2.82	-3647	3534
Δ^1J_{2-1}			91
Z_{tri}	3.14	-3642	3533
$Z_2\text{tri}$	4.48	-3659	3621
Δ^1J_{2-1}			88
$Z_3\text{tri}$	5.85	-3682	3694
Δ^1J_{3-2}			73

^a $^1J(\text{Pt,P})$ values are in Hz; measurements were made at room temperature, except as indicated. ^b ^{31}P NMR spectra were measured at 36.43 MHz. ^c ^{195}Pt NMR spectra were measured at 53.5 MHz, and the values are relative to external Na_2PtCl_6 .

shift of the ^{31}P resonance. Coordination of more than one platinum fragment to the same heterocycle, however, results in a downfield shift of this resonance.

The ^{195}Pt chemical shifts move upfield on bridge splitting as well as on coordination of more than one platinum fragment to the same nitrogen heterocycle.

$^1J(\text{Pt,P})$ coupling constants for monocoordinated complexes of the type $\text{trans-PtCl}_2(\text{L}')(\text{PEt}_3)$ ($\text{L}' = \text{nitrogen donor ligand}$) generally lie in the range 3340–3550 Hz.²⁰ Z_{mon} , Z_{di} , and Z_{tri} show typical values for such complexes. However, $Z_2\text{di}$, $Z_2\text{tri}$, and $Z_3\text{tri}$ possess higher values with 3568, 3621, and 3694 Hz,

Table III. ^1H NMR Chemical Shifts (δ) for the Aromatic Protons^a of the Ligands L and Their Complexes $Z_n\text{L}$ (L = mon, di, and tri)


complex	H(2)	H(3), H(5)	H(4)	H(6)
mon	8.57	7.26	7.67	8.57
Zmon	8.87	7.43	7.85	8.87
$\Delta\delta(\text{mon})^b$	+0.30	+0.17	+0.18	+0.30
di	9.15	7.30	8.69	8.69
Zdi	9.55	7.47	8.84	9.14
$\Delta\delta(\text{di})_1^c$	+0.40	+0.17	+0.15	+0.45
Z ₂ di	10.08	7.61	9.37	9.37
$\Delta\delta(\text{di})_2^d$	+0.53	+0.14	+0.53	+0.23
tri	9.18		9.18	9.18
Ztri	9.69		9.31	9.69
$\Delta\delta(\text{tri})_1^e$	+0.51		+0.13	+0.51
Z ₂ tri	10.33		9.89	9.89
$\Delta\delta(\text{tri})_2^f$	+0.64		+0.58	+0.20
Z ₃ tri	10.56		10.56	10.56
$\Delta\delta(\text{tri})_3^g$	+0.23		+0.67	+0.67

^aSpectra recorded at 90 MHz in CD_2Cl_2 solution at room temperature except for $Z_3\text{tri}$ (measured at 0 °C). The proton numbering in the complexes is such that when one platinum atom is coordinated this occupies position 1 and when two of them are present these occupy positions 1 and 3. ^b $\Delta\delta(\text{mon}) = \delta(\text{Zmon}) - \delta(\text{mon})$. ^c $\Delta\delta(\text{di})_1 = \delta(\text{Zdi}) - \delta(\text{di})$. ^d $\Delta\delta(\text{di})_2 = \delta(\text{Z}_2\text{di}) - \delta(\text{Zdi})$. ^e $\Delta\delta(\text{tri})_1 = \delta(\text{Ztri}) - \delta(\text{tri})$. ^f $\Delta\delta(\text{tri})_2 = \delta(\text{Z}_2\text{tri}) - \delta(\text{Ztri})$. ^g $\Delta\delta(\text{tri})_3 = \delta(\text{Z}_3\text{tri}) - \delta(\text{Z}_2\text{tri})$.

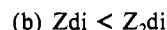
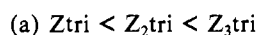
respectively. As can be seen in Table II, there is a trend toward increasing values of the coupling constants upon moving to a higher number of coordinated Z units, ΔJ being typically 70–100 Hz. Such a trend can also be observed for the corresponding complexes with unsubstituted and symmetrically substituted pyrazine complexes, although there the ΔJ values are somewhat smaller (40–70 Hz).²¹

Although the numerical differences between the $^1J(\text{Pt},\text{P})$ values of the complexes reported here are rather small, two main trends are observable:

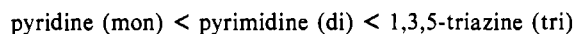
(1) The J values increase in the series



(2) They also increase in the series



The first observation may be related to the increasing s character of the nitrogen atom(s) in the series²²



The second observation indicates that if an increase in s character of the nitrogen donor is responsible for the observed increase in $^1J(\text{Pt},\text{P})$ for the bond in a position trans to the N donor, the s character of each nitrogen atom in 1,3,5-triazine increases as successive platinum atoms are coordinated to this ligand. These effects, however, would be too small to be observable given the standard deviations for the Pt–N bond lengths (see Crystal Structure of $Z_3\text{tri}$).

^1H NMR Spectra. These data for the ligands L and their complexes of the types $Z_n\text{L}$ (L = mon, di, and tri) are listed in Tables III and IV. The above data show that all the δ values move to lower fields on complex formation. The $\Delta\delta$ values ($\delta_{\text{complex}} - \delta_{\text{free ligand}}$) depend on the number of platinum atoms present in the complex and on the proximity of the proton in question to one or more metal centers.

Table IV. Coupling Constants for the Aromatic Protons^a in the Ligands L and Their Complexes $Z_n\text{L}$

	Zmon	Zdi	Z ₂ di	Ztri ^b	Z ₂ tri	Z ₃ tri
$^3J(\text{N}(2),\text{H}(3))$	5.15					
$^4J(\text{H}(2),\text{H}(4))$	1.55	0.22	0.81	0.70	1.35	1.50
$^5J(\text{H}(2),\text{H}(5))$	0.90	1.00	1.06			
$^4J(\text{H}(2),\text{H}(6))$	0.60	1.00	0.81	<i>c</i>	1.35	1.50
$^3J(\text{H}(3),\text{H}(4))$	7.71					
$^4J(\text{H}(3),\text{H}(5))$	1.30					
$^5J(\text{H}(3),\text{H}(6))$	0.90					
$^3J(\text{H}(4),\text{H}(5))$	7.71	5.14	5.65			
$^4J(\text{H}(4),\text{H}(6))$	1.55	2.95	2.85	0.70	1.21	1.50
$^3J(\text{H}(5),\text{H}(6))$	5.15	5.85	5.65			
$^4J(\text{P},\text{H}(2))$	2.80	1.35	1.50	1.28	1.56	1.567
$^5J(\text{P},\text{H}(3))$	0.335					
$^4J(\text{P},\text{H}(4))$			2.70		1.22	1.567
$^6J(\text{P},\text{H}(4))$	0	0	0	0.625	0.40	0
$^5J(\text{P},\text{H}(5))$	0.335	0.67	1.02			
$^4J(\text{P},\text{H}(6))$	2.80	2.24	2.70	1.28	1.22	1.567
$^6J(\text{P},\text{H}(6))$			0		0.40	0
$^3J(\text{Pt},\text{H}(2))^d$	22.3	14.0	16.1	14.9	14.6	15.2
$^3J(\text{Pt},\text{H}(4))^d$			20.9		12.7	15.2
$^3J(\text{Pt},\text{H}(6))^d$	22.3	21.6	20.9	14.9	12.7	15.2

^aAll coupling constants are in Hz. For the proton numbering, see Table III. The $J(\text{H},\text{H})$ and $J(\text{P},\text{H})$ coupling constants were verified by homonuclear decoupling and simulation experiments. ^bWhen the spectrum of this compound was recorded at –60 °C, a $^5J(\text{Pt},\text{H}(4))$ coupling constant of 4.3 Hz was observed. ^cThe value of $^4J(\text{H}(2),\text{H}(6))$ in this compound could not be determined either by homonuclear decoupling or by simulation experiments. ^dNo $^4J(\text{Pt},\text{H})$ coupling constants could be observed.

As shown in Table III, coordination of a Z fragment to N(1) of triazine causes a downfield shift of the proton resonances. This is large (ca. 0.5 ppm) for the “2,6-protons”, H(2) and H(6), and small (ca. 0.1 ppm) for the “4-proton”, H(4). Coordination of a second Z unit to the N(3) atom of triazine causes a further downfield shift of the resonances. This is (a) 0.64 ppm for H(2), which is now in a position adjacent to two platinum atoms, (b) 0.58 ppm for H(4), which has now acquired one platinum atom in an adjacent position, and (c) 0.20 ppm for H(6), which has now acquired one platinum atom in the 3-position. Addition of the third Z unit to triazine causes further downfield shifts as follows: (a) an amount of ca. 0.2 ppm for H(2), which has now acquired a platinum atom in the 5-position, and (b) one of ca. 0.7 ppm for H(4) and H(6), both of them having acquired another platinum atom in an adjacent position. Thus, these changes are additive, i.e., a shift of 0.6–0.7 ppm for an adjacent platinum and ca. 0.2 ppm for a platinum atom in a position on the opposite side of the ring. Just like triazine, pyrimidine (di) shows downfield shifts for all protons upon coordination and, as expected, H(2) exhibits the largest overall shift difference (0.93 ppm), while the overall difference for H(5) remains comparatively small (0.31 ppm). The values of the $^3J(\text{Pt},\text{H})$ coupling constants are strongly dependent upon the nature of the neighboring atoms (see Table IV); i.e., those that are in a position adjacent to two nitrogen atoms have a coupling constant (14.0–14.9 Hz) smaller than that for those atoms adjacent only to the coordinated nitrogen (20.9–22.3 Hz). Coordination of second or third Z units does not significantly influence $^3J(\text{Pt},\text{H})$ values. The coupling constant for H(2) in $Z_2\text{di}$ is 2.1 Hz larger than in $Z\text{di}$, while $^3J(\text{Pt},\text{H})$ for H(6) remains essentially unchanged. On the other hand, the ΔJ value for H(6) as one goes from $Z\text{tri}$ to $Z_2\text{tri}$ is –2.2 Hz, and for H(4) and H(6) as one goes from $Z_2\text{tri}$ to $Z_3\text{tri}$ it is +2.5 Hz. $^4J(\text{Pt},\text{H})$ coupling constants could not be determined in any of the complexes, due to the fact that Pt satellites disappear under the main signal. As mentioned earlier, there is a marked sharpening of proton signals upon reducing the temperature (see Figure 3). This effect runs parallel to another; i.e., protons located in a position adjacent to a coordinated nitrogen atom display a pronounced upfield shift upon a lowering of the temperature (see Table V and Figures 3 and 5). There are a number of contributing factors causing chemical shift differences. Thus, when the complex is cooled, the nitrogen ligand spends a larger amount of time in the proximity

(21) Kaufmann, W.; et al., to be submitted for publication.

(22) Quirke, J. M. E. *Comprehensive Heterocyclic Chemistry*; Pergamon: Oxford, England, 1984; Vol. 3, Part 2B, p 7.

Table V. Temperature Dependence of the Chemical Shifts (δ) of the Aromatic Protons in the Complexes Z_nL ($L = \text{mon, di, tri}$) in CD_2Cl_2

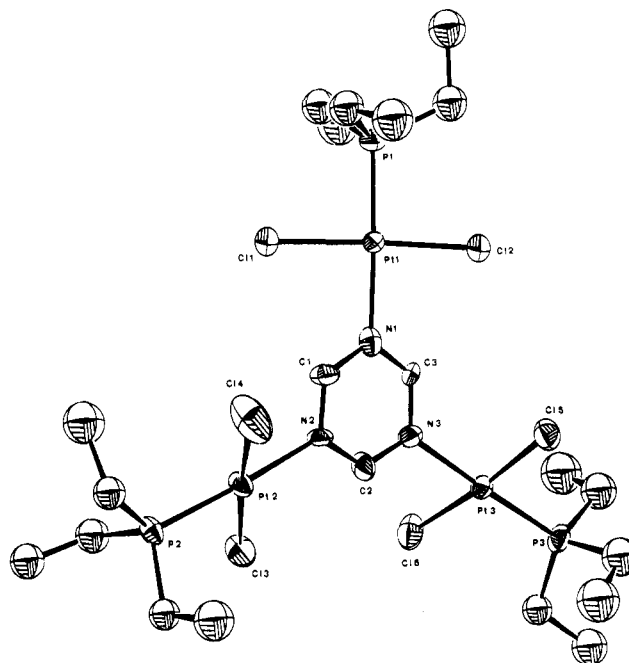
Zmon				
temp, °C	H(2,6)	H(3,5)	H(4)	
+27	8.87	7.43	7.85	
-60	8.76	7.43	7.85	
$\Delta\delta$	-0.11	0	0	
Zdi				
temp, °C	H(2)	H(4)	H(5)	H(6)
+27	9.55	8.84	7.47	9.14
-60	9.45	8.84	7.49	9.06
$\Delta\delta$	-0.10	0	+0.02	-0.08
Z ₂ di				
temp, °C	H(2)	H(4,6)	H(5)	
+27	10.08	9.37	7.61	
-60	9.88	9.24	7.65	
$\Delta\delta$	-0.20	-0.13	+0.04	
Ztri				
temp, °C	H(2,6)	H(4)		
+27	9.69	9.31		
-60	9.61	9.32		
$\Delta\delta$	-0.08	+0.01		
Z ₂ tri				
temp, °C	H(2)	H(4,6)		
+27	10.33	9.89		
-60	10.14	9.82		
$\Delta\delta$	-0.19	-0.07		
Z ₃ tri				
temp, °C	H(2,4,6)			
0	10.56			
-60	10.42			
$\Delta\delta$	-0.14			

of a given metal center, resulting in an electronic effect. Furthermore, one must consider a rotational factor caused by the angle formed between the ligand and the plane defined by the platinum, phosphorus, and chlorine atoms. Finally, there is an anisotropic effect due to the two chlorine atoms located in the cis positions with respect to the nitrogen ligand. It is, therefore, practically impossible to give a reliable explanation for the observed changes.

It has been known for some time that pyridine is not very strongly bonded in compounds of the type *trans*-PtCl₂(mon)(L), where L is a ligand of high trans effect.^{23,24} NMR studies of such complexes have focused primarily on compounds with L = CO, acetylene, and olefins, and there seems to have been only slight investigation of complexes with L = tertiary phosphines, even though these exert a moderately high trans effect.¹⁵ One would expect pyrimidine and triazine to behave in a manner similar to that of pyridine. We believe that our NMR studies show that this is actually the case.

Finally, it should be pointed out that the bonding of one Z fragment to pyrimidine or triazine appears to be very similar to that of pyridine to the same unit, as the appropriate ³J(Pt,H) values are comparable.

Crystal Structure of Z₃tri. An ORTEP view of the molecule with the atomic numbering scheme is given in Figure 10, and a selection of bond lengths and angles is given in Table VI. The structure consists of three square-planar platinum atoms, each coordinated to one nitrogen of the triazine molecule. Each square-planar unit shows normal coordination features, and the bond lengths and

**Figure 10.** ORTEP view of $\{\text{PtCl}_2(\text{PEt}_3)_3\}\text{triazine}$ ($Z_3\text{tri}$).**Table VI.** Relevant Bond Lengths (Å), Bond Angles (deg), and Torsion Angles (deg) for $Z_3\text{tri}$ ($Z = \text{PtCl}_2(\text{PEt}_3)$)^a

Pt(1)-Cl(1)	2.269 (6)	Pt(2)-P(2)	2.223 (5)
Pt(1)-Cl(2)	2.296 (5)	Pt(2)-N(2)	2.15 (1)
Pt(1)-P(1)	2.219 (5)	Pt(3)-Cl(5)	2.294 (6)
Pt(1)-N(1)	2.15 (1)	Pt(3)-Cl(6)	2.302 (6)
Pt(2)-Cl(3)	2.287 (4)	Pt(3)-P(3)	2.230 (3)
Pt(2)-Cl(4)	2.291 (6)	Pt(3)-N(3)	2.12 (1)
Cl(2)-Pt(1)-N(1)	88.7 (3)	P(3)-Pt(3)-N(3)	176.4 (5)
P(2)-Pt(2)-N(2)	174.2 (5)	Cl(5)-Pt(3)-Cl(6)	174.7 (2)
Cl(3)-Pt(2)-Cl(4)	173.9 (2)	Cl(5)-Pt(3)-P(3)	90.9 (2)
Cl(3)-Pt(2)-P(2)	89.2 (2)	Cl(6)-Pt(3)-P(3)	94.2 (2)
Cl(4)-Pt(2)-P(2)	94.4 (2)	Cl(5)-Pt(3)-N(3)	85.7 (4)
Cl(3)-Pt(2)-N(2)	88.4 (3)	Cl(6)-Pt(3)-N(3)	89.2 (4)
Cl(4)-Pt(2)-N(2)	88.5 (4)	Pt(1)-Pt(1)-N(1)	177.4 (6)
Pt(1)-N(1)-C(1)	120.9 (7)	Cl(1)-Pt(1)-Cl(2)	174.8 (2)
Pt(1)-N(1)-C(3)	122.6 (7)	Cl(1)-Pt(1)-P(1)	94.1 (2)
Pt(2)-N(2)-C(1)	119.7 (7)	Cl(2)-Pt(1)-P(1)	89.2 (2)
Pt(2)-N(2)-C(2)	124.4 (7)	Cl(1)-Pt(1)-N(1)	88.1 (4)
Pt(3)-N(3)-C(2)	120.3 (8)	C(1)-N(1)-Pt(1)-Cl(2) ^b	35.2
Pt(3)-N(3)-C(3)	123.7 (6)	C(1)-N(2)-Pt(2)-Cl(4)	43.3
		C(2)-N(3)-Pt(3)-Cl(6)	-60.3

^a Esd's in the last significant digit are given in parentheses. ^b Esd's in torsion angles are in the range 0.6–0.8°.

angles fall within the range of those found for complexes of the type *trans*-PtCl₂(N-ligand)(PR₃).²⁵ A possible exception is the Pt-N bond length, which is slightly longer than those observed in a number of pyridine complexes.²⁵ The differences, however, are small and fall within the limits of accuracy of the structure determination. The triazine ring in $Z_3\text{tri}$ is planar, and the C=N bonds (average 1.34 (2) Å) and N-C-N (average 124.1 (9)°) and C-N-C bond angles (average 115.8 (7)°) are equal to those found in the free ligand.²⁶ It should be noted that the three platinum atoms are coplanar with the ring, the maximum deviation from the least-squares plane for the ring being 0.2 Å.

The bond distances and angles at each square-planar platinum atom are comparable with those observed in *trans*-dichloro-

(23) Kaplan, P. D.; Schmidt, P.; Orchin, M. *J. Am. Chem. Soc.* **1968**, *90*, 4175.

(24) Orchin, M.; Schmidt, P. *J. Inorg. Chim. Acta, Rev.* **1968**, *2*, 123.

(25) Albinati, A.; Anklin, C. G.; Ganazzoli, F.; Rügge, H.; Pregosin, P. S. *Inorg. Chem.* **1987**, *26*, 503.

(26) Coppens, P. *Science (Washington, D.C.)* **1967**, *158*, 1577.

(quinoline-8-carbaldehyde)(triethylphosphine)platinum(II) (2.160 (2) Å).²⁶ Thus, the Pt–N bond distances in the triazine complex (average 2.14 (1) Å) are comparable with the Pt–N distance of 2.102 (7) Å in *trans*-dichloro(2-((2,4,6-trimethylbenzylidene)amino)-3-methylpyridine)(triethylarsine)platinum(II) and of 2.155 (5) Å in *trans*-dichloro(2-amino-3-methylpyridine)(triethylphosphine)palladium(II).²⁷ It should be noted that these Pt–(Pd)–N distances represent the upper range of values (average 2.02 (1) Å) reported in the literature and may be due to the presence of a P (As) donor in a position *trans* to nitrogen.²⁸ The remarkable feature of this structure is the near-normal length of the Pt–N bonds of triazine, which is simultaneously bonded to three platinum atoms. On this basis it can be deduced that each Pt–N bond is of strength comparable to that in a complex with a mononitrogen heterocycle such as pyridine. This observation provides support for the earlier postulate that the binding of platinum fragments such as “PtCl₂(PEt₃)” does not significantly weaken the electron donor capacity of the remaining free nitrogen atoms.

Experimental Section

Instrumentation. Proton NMR spectra were recorded either on a Bruker WH 90 or on a WM 250 spectrometer and ³¹P spectra on a Bruker HX 90 or WM 250 spectrometer. ¹³C and ¹⁹⁵Pt spectra were also obtained by the use of a WM 250 spectrometer. Either CDCl₃ or CD₂Cl₂ was used as a solvent. Solid-state ³¹P NMR spectra were recorded on a Bruker AC 250 spectrometer at 101 MHz with magic-angle spinning and high-power decoupling. Melting points were determined on a Büchi SMP 20 apparatus. IR spectra were recorded on a Perkin-Elmer 1430 or 883 infrared spectrometer, using KBr or CsI pellets or CD₂Cl₂ solutions. Elemental analyses were performed at the “Mikrolabor-ETH Zürich”.

Starting Materials. Triazine, pyrimidine, and pyridine (Fluka products) were used as received. CDCl₃ and CD₂Cl₂ were obtained from Stohler Isotope Chemicals. Other organic solvents (99%) were used without further purification. Pt₂Cl₄(PEt₃)₂ and Pt₂Cl₄(*P-n-Bu*)₂ were prepared as previously described.²⁹

Syntheses. General Procedure. A 0.26-mmol portion (or a fraction thereof, e.g. two-thirds or half, depending on the desired coordination complex and the number of N atoms per heterocycle) of triazine, pyrimidine, or pyridine was added to a solution of 0.13 mmol of Pt₂Cl₄(PR₃)₂ (R = Et, *n-Bu*) in 2.5 mL of CDCl₃, and the mixture was stirred for 5 min. The resulting greenish yellow solution was directly used for the NMR measurements. No attempts were made to isolate the *P-n-Bu*₃ complexes because of their very high solubility.

{PtCl₂(PEt₃)}₂tri (Ztri). Attempts to isolate the solid product from a solution in which Ztri was the predominant species yielded only greenish yellow oils, which, when dried under vacuum for a longer period of time, turned into semiviscous substances. CDCl₃ solutions thereof showed that they consisted primarily of Ztri with some Z₃tri. NMR: ¹³C (CDCl₃), δ 7.9, 14.9 (¹J(P,C) = 40.5 Hz), 166.3, 166.9. IR (CD₂Cl₂): 1579, 1554, 1404, 1043 cm⁻¹.

{PtCl₂(PEt₃)}₂tri (Z₂tri). Attempts to obtain crystalline Z₂tri from a solution (prepared as described in the General Procedure) by floating a layer of hexane on top of the CDCl₃ solution led to the formation of greenish yellow crystals of Z₃tri contaminated with a yellow oil, which contained mainly Ztri. However, if the CDCl₃ solution was taken to dryness under vacuum, a greenish yellow powder of composition Z₂tri was obtained: yield 92%; mp 135–136 °C. Anal. Calcd for C₁₅H₃₃N₃Cl₄P₂Pt₂: C, 21.21; H, 3.92; N, 4.95; Cl, 16.70. Found: C, 21.16; H, 3.98; N, 4.72; Cl, 16.76. NMR: ¹³C (CDCl₃), δ 7.9, 15.0 (¹J(P,C) = 40.9), 166.6. IR (KBr): 1574, 1564, 1412, 1039 cm⁻¹.

{PtCl₂(PEt₃)}₃tri (Z₃tri). A layer of hexane was floated on top of a CDCl₃ solution of this complex obtained as indicated in the General Procedure. When the solution stood at room temperature, intense yellow-green crystals of product were obtained in 90% yield; mp 157–158 °C. Anal. Calcd for C₂₁H₄₈N₃Cl₄P₃Pt₃: C, 20.45; H, 3.92; N, 3.41; Cl, 17.24. Found: C, 20.45; H, 3.97; N, 3.59; Cl, 17.64. NMR: ¹³C (CDCl₃, –60 °C), δ 7.8, 14.0 (¹J(P,C) = 41.1 Hz), 166.8. IR (KBr): 1579, 1561, 1413, 1039 cm⁻¹.

{PtCl₂(PEt₃)}₂di (Zdi). Attempts to obtain solid Zdi as described for Ztri gave only small amounts of crystalline Z₂di. Evaporation of the original solution, at room temperature, in vacuo yielded pure Z₂di in

nearly quantitative amounts as di sublimed during this process. NMR: ¹³C (CDCl₃), δ 7.9, 14.7 (¹J(P,C) = 40.7 Hz, ²J(Pt,C) = 32.3), 121.9, 157.6, 158.7, 159.8. IR (CD₂Cl₂): 1591, 1561, 1408, 1039 cm⁻¹.

{PtCl₂(PEt₃)}₂di (Z₃tri). Thin, light green needles were obtained in a yield of 88% as described for Z₃tri; mp 196 °C dec. Anal. Calcd for C₁₆H₃₄N₂Cl₄P₂Pt₂: C, 22.65; H, 4.04; N, 3.30; Cl, 16.71. Found: C, 22.80; H, 4.01; N, 3.42; Cl, 16.98. NMR: ¹³C (CDCl₃), δ 7.9, 14.9 (¹J(P,C) = 41.1 Hz, ²J(Pt,C) = 33.4 Hz), 122.0, 159.0, 161.2. IR (KBr): 1598, 1591, 1407, 1037 cm⁻¹.

{PtCl₂(*P-n-Bu*)₂}₂di. NMR: ¹H (CDCl₃, 90 MHz), δ 0.95 (app t, 18 H, PCH₂CH₂CH₂CH₃), 1.2–2.2 (m, 36 H, PCH₂CH₂CH₂CH₃), 7.53 (m, 1 H, H(5)), 9.37 (m, 2 H, H(4) and H(6)), 10.17 (m, ³J(Pt,H) = 15.8 Hz, 1 H, H(2)); ³¹P{¹H} (CDCl₃, 36.43 MHz), δ –5.13 (¹J(Pt,P) = 3518 Hz).

***trans*-PtCl₂(mon)(PEt₃) (Zmon).**¹⁸ Recrystallization of the crude product from chloroform/hexane produced thin, light green needles in 90% yield; mp 87 °C. Anal. Calcd for C₁₁H₂₀NCl₂PPt: C, 28.52; H, 4.35; N, 3.02; Cl, 15.31. Found: C, 28.88; H, 4.49; N, 2.92; Cl, 15.19. NMR: ¹³C (CDCl₃), δ 7.9, 14.8 (¹J(P,C) = 39.7 Hz, ²J(Pt,C) = 31.4 Hz), 125.3 (³J(Pt,C) = 23.2 Hz, ⁴J(P,C) = 3.2 Hz), 138.8 (⁴J(Pt,C) = 5.7 Hz), 151.1 (²J(Pt,C) = 11.5 Hz). IR (CsI): 1604, 1447, 1038 cm⁻¹.

***trans*-PtCl₂(mon)(*P-n-Bu*)₃.** NMR: ¹H (CDCl₃, 90 MHz), δ 0.96 (app t, 9 H, PCH₂CH₂CH₂CH₃), 1.2–2.1 (m, 18 H, PCH₂CH₂CH₂CH₃), 7.37 (m, 2 H, H(3) and H(5)), 7.79 (m, 1 H, H(4)), 8.91 (m, ³J(Pt,H) = 22 Hz, 2 H, H(2) and H(6)); ³¹P{¹H} (CDCl₃, 36.43 MHz), δ –8.24 (¹J(Pt,P) = 3339 Hz).

***trans*-PtCl₂(4-Cl-mon)(PEt₃).** 4-Chloropyridine was obtained by deprotonation of the corresponding hydrochloride with 0.5 g of sodium carbonate in 2.5 mL of CDCl₃. Pt₂Cl₄(PEt₃)₄ was added directly to this mixture, which was stirred vigorously for 4 h until its color changed from orange to a pale greenish yellow. Filtration followed by evaporation of the resulting solution yielded 88% of the above product; mp 103 °C. Anal. Calcd for C₁₁H₉NCl₃PPt: C, 26.55; H, 3.85; N, 2.81; Cl, 21.37. Found: C, 26.60; H, 3.89; N, 2.69; Cl, 21.41. NMR: ¹H (CDCl₃, 90 MHz), δ 1.21 (dt, J(H,H) = 7.6 Hz, ³J(P,H) = 17.2 Hz, 9 H, PCH₂CH₃), 1.95 (dq, J(H,H) = 7.6 Hz, ²J(P,H) = 11.1 Hz, 6 H, PCH₂CH₃), 7.40 (m, 2 H, H(3) and H(5)), 8.86 (m, ³J(Pt,H) = 22.2 Hz, 2 H, H(2) and H(6)); ¹³C (CDCl₃), δ 7.9, 14.7 (¹J(P,C) = 39.6 Hz), 125.6, 147.0, 151.6; ³¹P (CDCl₃, 36.43 MHz), δ 0.44 (¹J(Pt,P) = 3391 Hz). IR (KBr): 1592, 1480, 1453, 1413, 1038 cm⁻¹. The proton numbering scheme is based upon that given in Table II for pyridine.

***trans*-PtCl₂(4-Cl-mon)(*P-n-Bu*)₃.** NMR: ¹H (CDCl₃, 90 MHz), δ 0.96 (app t, 9 H, PCH₂CH₂CH₂CH₃), 1.2–2.1 (m, 18 H, PCH₂CH₂CH₂CH₃), 7.39 (m, 2 H, H(3) and H(5)), 8.85 (m, ³J(Pt,H) = 22.2 Hz, 2 H, H(2) and H(6)); ³¹P{¹H} (CDCl₃, 36.43 MHz), δ –7.39 (¹J(Pt,P) = 3375 Hz).

Exchange Reactions. General Procedure. Equimolar amounts (0.06 mmol) of the two compounds were dissolved separately in CDCl₃; the solutions were mixed and immediately measured spectroscopically.

(A) {PtCl₂(PEt₃)}₂di and Pt₂Cl₄(*P-n-Bu*)₂. NMR: ³¹P{¹H} (CDCl₃, 36.43 MHz), δ –5.31 (¹J(Pt,P) = 3518 Hz, {PtCl₂(*P-n-Bu*)₂}₂di, {PtCl₂(*P-n-Bu*)₃}[PtCl₂(PEt₃)]₂di}, 2.38 (¹J(Pt,P) = 3819 Hz, ³J(Pt,P) = 21 Hz, Pt₂Cl₄(*P-n-Bu*)₂, Pt₂Cl₄(*P-n-Bu*)₃(PEt₃)), 2.78 (¹J(Pt,P) = 3536 Hz, {PtCl₂(PEt₃)}₂di, {PtCl₂(*P-n-Bu*)₃}[PtCl₂(PEt₃)]₂di}, 10.33 (¹J(Pt,P) = 3842 Hz, ³J(Pt,P) = 24 Hz, Pt₂Cl₄(PEt₃)₂, Pt₂Cl₄(*P-n-Bu*)₃(PEt₃)).

(B) Pt₂Cl₄(*P-n-Bu*)₂ and Pt₂Cl₄(PEt₃)₂. NMR: ³¹P{¹H} (CDCl₃, 101.3 MHz), δ 9.74 (¹J(Pt,P) = 3848 Hz, Pt₂Cl₄(PEt₃)₂), 9.68 (¹J(Pt,P) = 3848 Hz, Pt₂Cl₄(*P-n-Bu*)₃(PEt₃)), 1.86 (¹J(Pt,P) = 3828 Hz, Pt₂Cl₄(*P-n-Bu*)₃(PEt₃)), 1.78 (¹J(Pt,P) = 3828 Hz, Pt₂Cl₄(*P-n-Bu*)₂).

(C) *trans*-PtCl₂(mon)(PEt₃) and Pt₂Cl₄(*P-n-Bu*)₂. NMR: ³¹P{¹H} (CDCl₃, 36.43 MHz), δ 10.29 (¹J(Pt,P) = 3842 Hz, Pt₂Cl₄(PEt₃)₂), 10.21 (¹J(Pt,P) = 3842 Hz, Pt₂Cl₄(*P-n-Bu*)₃(PEt₃)₂), 2.46 (¹J(Pt,P) = 3822 Hz, Pt₂Cl₄(*P-n-Bu*)₃(PEt₃)₂), 2.34 (¹J(Pt,P) = 3822 Hz, Pt₂Cl₄(*P-n-Bu*)₂), –0.41 (¹J(Pt,P) = 3352 Hz, *trans*-PtCl₂(mon)(PEt₃)), –8.24 (¹J(Pt,P) = 3339 Hz, *trans*-PtCl₂(mon)(*P-n-Bu*)₃).

(D) *trans*-PtCl₂(mon)(*P-n-Bu*)₃ and *trans*-PtCl₂(4-Cl-mon)(PEt₃). A solution containing 0.1 mmol of *trans*-PtCl₂(mon)(*P-n-Bu*)₃ in CDCl₃, obtained by the previously described method, was added to a solution containing 0.1 mmol of PtCl₂(4-Cl-mon)(PEt₃) in CDCl₃. Spectroscopical measurements indicated that the reaction had reached equilibrium after 20 min. NMR: ³¹P{¹H} (CDCl₃, 36.43 MHz), δ 0.44 (¹J(Pt,P) = 3391 Hz, *trans*-PtCl₂(4-Cl-mon)(PEt₃)), –0.37 (¹J(Pt,P) = 3352 Hz, *trans*-PtCl₂(mon)(PEt₃)), –7.39 (¹J(Pt,P) = 3375 Hz, *trans*-PtCl₂(4-Cl-mon)(*P-n-Bu*)₃), –8.20 (¹J(Pt,P) = 3336 Hz, *trans*-PtCl₂(mon)(*P-n-Bu*)₃).

X-ray Measurements. Crystals suitable for X-ray diffraction of Z₃tri were obtained by slow diffusion of hexane into a chloroform solution of Z₃tri and are air-stable. A prismatic crystal was mounted on a glass fiber at a random orientation on a Nonius CAD4 diffractometer for the data

(27) Albinati, A.; Arz, C.; Pregosin, P. S. *Inorg. Chem.* **1987**, *26*, 508.

(28) Palenik, G. J.; Giordano, T. J. *J. Chem. Soc., Dalton Trans.* **1987**, 1175.

(29) Goodfellow, R. J.; Venanzi, L. M. *J. Chem. Soc.* **1965**, 7533.

Table VII. Experimental Data^a for the X-ray Diffraction Study of Z₃tri

formula	Pt ₃ Cl ₆ P ₃ N ₃ C ₂₁ H ₄₈
<i>M_r</i>	1233.55
cryst dimens, mm	0.1 × 0.2 × 0.2
cryst syst	triclinic
space group	<i>P</i> $\bar{1}$
<i>a</i> , Å	13.020 (2)
<i>b</i> , Å	13.098 (2)
<i>c</i> , Å	13.251 (2)
α , deg	62.75 (1)
β , deg	65.95 (2)
γ , deg	75.49 (2)
<i>Z</i>	2
<i>V</i> , Å ³	1828.8 (1)
ρ (calcd), g cm ⁻³	2.239
μ , cm ⁻¹	122.0
radiation	Mo K α (graphite monochromated)
no. of measd reflns	4740
θ range, deg	2.0 ≤ θ ≤ 24.5
scan type	$\omega/2\theta$
max scan speed, deg min ⁻¹	10.2
scan width, deg	1.0 + 0.35 tan θ
max counting time, s	60
prescan rejection line	0.5 (2 σ)
prescan acceptance line	0.025 (40 σ)
bkgd time	0.5 × scan time
horiz receiving aperture, mm	1.9 + tan θ
vert receiving aperture, mm	4.0
no. of data collected	4740 ($\pm h, \pm k, +l$)
no. of data used in refinement ($ F_o > 2.5\sigma(F_o)$)	3944
<i>R</i> ^b	0.036
<i>R_w</i> ^c	0.041

^aData collected at room temperature. ^b $R = \sum ||F_o| - |F_c|| / \sum |F_o|$.
^c $R_w = [\sum w(|F_o| - |F_c|)^2 / \sum wF_o^2]^{1/2}$.

collection. Cell constants were obtained by a least-squares fit of the 2 θ values of 25 high-angle reflections (10.0 ≤ θ ≤ 15.0°) with the CAD4 centering routine.³⁰ Crystallographic and data collection parameters are given in Table VII. Data were collected by using an $\omega/2\theta$ scan technique with variable scan speed to obtain constant statistical precision on the collected intensities. Three standard reflections ($\bar{5}11, 51\bar{1}, 10\bar{6}$) were measured every 1 h and used to check the stability of the crystal and of the experimental conditions; no significant variation was detected. The orientation of the crystal was checked by measuring three reflections ($\bar{5}11, 7\bar{1}3, 10\bar{6}$) every 300 reflections. Data were corrected for Lorentz and polarization factors and absorption with the data reduction programs of the CAD4-SDP package;³⁰ $I_{net} = 0.0$ was given to those reflections having negative net intensities. An empirical absorption correction was applied by using the azimuthal (Ψ) scans of the high- χ -angle reflections $144, 155, 288$, and $19,10$. Transmission factors were in the range 0.447–0.998. Reflections having $F_o \geq 2.5\sigma(F_o)$ were considered as observed and used for the solution and refinement of the structure. The structure was solved by Patterson and Fourier methods and refined by a block-diagonal least-squares procedure³¹ (the function minimized was $(\sum w(|F_o| - (1/k)|F_c|)^2)$ with weights obtained from a Cruickshank scheme³² by demanding that no systematic trend be present in the weights with $|F_o|$ or $(\sin \theta)/\lambda$. No extinction correction was applied. The scattering factors used, corrected for anomalous dispersion,³³ were taken from

Table VIII. Final Positional Parameters for Z₃tri

	<i>x/a</i>	<i>y/b</i>	<i>z/c</i>
Pt(1)	0.242 24 (5)	0.129 90 (4)	0.260 69 (6)
Pt(2)	0.214 00 (5)	0.427 22 (5)	0.510 59 (5)
Pt(3)	0.299 98 (5)	0.641 78 (5)	-0.029 87 (5)
Cl(1)	0.158 89 (45)	0.217 60 (35)	0.117 64 (42)
Cl(2)	0.314 26 (38)	0.050 25 (33)	0.415 11 (37)
Cl(3)	0.351 14 (36)	0.554 31 (36)	0.401 12 (35)
Cl(4)	0.066 08 (49)	0.313 53 (54)	0.607 11 (41)
Cl(5)	0.146 67 (34)	0.587 90 (35)	-0.032 17 (36)
Cl(6)	0.455 52 (35)	0.678 78 (38)	-0.014 40 (39)
P(1)	0.241 46 (35)	-0.045 72 (31)	0.275 61 (36)
P(2)	0.209 72 (32)	0.431 26 (35)	0.678 17 (33)
P(3)	0.308 17 (34)	0.797 47 (33)	-0.200 57 (34)
N(1)	0.249 62 (94)	0.297 17 (97)	0.248 52 (103)
N(2)	0.235 19 (90)	0.415 49 (93)	0.346 78 (99)
N(3)	0.281 90 (90)	0.492 96 (94)	0.133 44 (99)
C(1)	0.229 17 (116)	0.314 37 (121)	0.348 96 (129)
C(2)	0.264 87 (120)	0.502 39 (126)	0.236 42 (132)
C(3)	0.273 72 (104)	0.387 64 (107)	0.145 61 (114)
C(11)	0.134 78 (153)	-0.123 55 (159)	0.410 70 (168)
C(21)	0.014 32 (187)	-0.075 09 (194)	0.413 13 (205)
C(31)	0.372 31 (156)	-0.136 29 (160)	0.284 99 (170)
C(41)	0.475 99 (202)	-0.088 39 (210)	0.167 94 (222)
C(51)	0.214 37 (152)	-0.047 45 (158)	0.148 28 (168)
C(61)	0.208 36 (173)	-0.174 33 (179)	0.167 41 (189)
C(12)	0.151 88 (133)	0.572 33 (138)	0.684 79 (146)
C(22)	0.028 09 (180)	0.605 62 (186)	0.681 83 (199)
C(32)	0.354 21 (150)	0.408 60 (156)	0.686 33 (166)
C(42)	0.358 46 (152)	0.399 70 (158)	0.803 40 (167)
C(52)	0.126 24 (137)	0.327 46 (141)	0.821 27 (150)
C(62)	0.177 96 (187)	0.199 32 (192)	0.839 71 (204)
C(13)	0.172 66 (172)	0.860 14 (179)	-0.216 56 (191)
C(23)	0.094 49 (211)	0.900 52 (217)	-0.111 05 (231)
C(33)	0.379 08 (136)	0.912 46 (140)	-0.221 66 (148)
C(43)	0.385 65 (167)	1.023 58 (171)	-0.339 17 (182)
C(53)	0.375 44 (167)	0.759 24 (174)	-0.330 66 (184)
C(63)	0.493 64 (205)	0.712 94 (213)	-0.347 38 (222)

tabulated values.³³ Anisotropic temperature factors were used for Pt and P atoms and for the atoms of the triazine ring, while isotropic thermal parameters were used for the remaining carbon atoms. The contribution of the hydrogen atoms in their idealized positions (C–H = 0.95 Å, $B_{iso} = 6.0 \text{ \AA}^2$) was also taken into account but not refined. Upon convergence (no shifts $\geq 0.4\sigma$) the last Fourier difference map showed no significant features. Final positional parameters are listed in Table VIII.

Acknowledgment. W.K. carried out the work during the tenure of a research fellowship from the Swiss National Research Council. A.A. acknowledges the support of the Italian National Research Council. We are greatly indebted to Dr. P. S. Pregosin for much valuable discussion and Dr. H. Rügger for the solid-state NMR measurements.

Registry No. Ztri, 112793-15-4; Z₂tri, 112793-16-5; Z₃tri, 112793-17-6; Zdi, 112793-18-7; Z₂di, 112793-19-8; Zmon, 52659-92-4; {PtCl₂(P-*n*-Bu₃)₂}di, 112793-20-1; *trans*-PtCl₂(mon)(P-*n*-Bu₃), 15282-35-6; *trans*-PtCl₂(4-Cl-mon)(PEt₃), 112793-21-2; *trans*-PtCl₂(4-Cl-mon)(P-*n*-Bu₃), 112793-22-3; Pt₂Cl₄(PEt₃)₂, 15692-96-3; Pt₂Cl₄(P-*n*-Bu₃)₂, 59421-67-9; {[PtCl₂(PEt₃)] [PtCl₂(P-*n*-Bu₃)] [di]}, 112793-23-4; Pt₂Cl₄(P-*n*-Bu₃)(PEt₃), 112793-24-5; ¹⁹⁵Pt, 14191-88-9.

Supplementary Material Available: Figure S1 (numbering scheme), Table S1 (positional and thermal factors), and Table S3 (list of bond distances and angles) (4 pages); Table S2 (listing of F_o and F_c) (27 pages). Ordering information is given on any current masthead page.

(30) *Enraf-Nonius Structure Determination Package, SDP*; Enraf-Nonius: Delft, The Netherlands, 1980.

(31) For reference to least-squares, Fourier, and structure factor calculation programs see: Albinati, A.; Brückner, S. *Acta Crystallogr., Sect. B: Struct. Crystallogr. Cryst. Chem.* **1978**, *B34*, 3390.

(32) Cruickshank, D. W. J. In *Computing Methods in Crystallography*; Ahmed, A., Ed.; Munksgaard: Copenhagen, 1972.

(33) *International Tables for X-Ray Crystallography*; Kynoch: Birmingham, England, 1974; Vol. IV.